PREPRINT UCRL- 79127

Lawrence Livermore Laboratory

LASER LIGHT ABSORPTION AND HARMONIC GENERATION DUE TO SELF-GENERATED MAGNETIC FIELDS

W. L. Kruer and K. G. Estabrook

February 1, 1977

This paper was prepared for presentation at the Fourth Workshop on "Laser Interaction and Related Plasma Phenomena" held at RPI, Troy, New York, November 8 - 12, 1976.

LASER LIGHT ABSORPTION AND HARMONIC GENERATION DUE TO SELF-GENERATED MAGNETIC FIELDS*†

W. L. Kruer and K. G. Estabrook

University of California, Lawrence Livermore Laboratory

Livermore, California 94550 U.S.

ABSTRACT

It is shown that self-generated magnetic fields can play a significant role in laser light absorption. Even normally incident light will then be resonantly absorbed. Computer simulations and theoretical estimates for this absorption and the concomitant harmonic generation are given for parameters characteristic of some recent experiments.

I. INTRODUCTION

It has been shown that self-generated dc magnetic fields[1-8] can strongly inhibit the electron heat flow in recent laser plasma experiments. In this paper we will show that these magnetic fields can also introduce an interesting amount of light absorption and harmonic generation. Physically the absorption and harmonic generation occurs due to electrostatic waves resonantly generated by the oscillation of electrons driven by the $\underline{v}_{os} \times \underline{B}_0/c$ force, where $\underline{v}_{os}$ is the quiver velocity of an electron in the laser light

*Presented at the Fourth Workshop on "Laser Interaction and Related Plasma Phenomena" held at RPI, Troy, New York, Nov. 8-12, 1976.

†Research performed under the auspices of the USERDA, Contract No. W-7405-Eng-48.

field and $\underline{B}_o$ is the self-generated dc magnetic field. In contrast to the resonance absorption[9-11] usually considered in laser-target applications, this mechanism is operative even for normally incident light. As we will show, the magnitude of the dc magnetic field which has been experimentally measured[2] ($B \sim 4$ MG) is large enough to make the light conversion to plasma waves sizeable, but not so large as to make the critical surface inaccessible to the light. In contrast, this mechanism is negligible for the case of radio waves in the ionosphere.[9]

Although the basic physical mechanism is of course well-known,[12] its application to laser-plasma targets is novel and potentially important. We here investigate this mode conversion process in a regime complementary to that studied in recent magnetic fusion applications.[13] In these latter applications, the electron cyclotron frequency (ω_{ce}) is > the electron plasma frequency (ω_{pe}), whereas in our applications $\omega_{ce} \ll \omega_{pe}$. For example, for $B = 4$ MG and a Nd laser, $\omega_{ce}/\omega_{pe} \approx .04$ at the critical density. Theoretical estimates for the coupling, saturation amplitudes, absorption, and harmonic generation will be given and explored in computer simulations for parameters characteristic of recent laser-plasma experiments. The calculations also show that the second harmonic generation may provide information both about the local scale length near the critical density and the size of the self-generated dc magnetic fields.

II. THEORETICAL ESTIMATES FOR THE MODE CONVERSION

The basic process will be investigated in a simple geometry. Let $\underline{B}_o = B_o \hat{x}$, and consider laser light normally incident ($\underline{k} = k(z)\hat{z}$) on a plasma with density $n = n(z)$. The electric vector of the light is orthogonal to $\underline{B}_o$ as it enters the plasma from vacuum. From Maxwell's equations and the linearized cold plasma equations, we can readily obtain coupled equations for E_y and E_z. Assuming a time-dependence of $e^{-i\omega_o t}$, we obtain

$$\frac{d^2E_y}{dz^2} = - \frac{\omega_o^2}{c^2} \varepsilon_1 E_y \qquad (1)$$

and

$$E_z = - \frac{\omega_{pe}^2}{\omega_o^2 - \omega_{ce}^2} \frac{i\omega_{ce}}{\omega_o} \frac{E_y}{\varepsilon_2} , \qquad (2)$$

where ε_1 and ε_2 are the dielectric functions:

$$\varepsilon_1 = 1 - \frac{\omega_{pe}^2}{\omega_0^2} \frac{(\omega_0^2 - \omega_{pe}^2)}{(\omega_0^2 - \omega_{UH}^2)} \quad (1)$$

and

$$\varepsilon_2 = 1 - \frac{\omega_{pe}^2}{\omega_0^2 - \omega_{ce}^2} . \quad (2)$$

Here ω_0 is the light frequency, ω_{pe} the local electron plasma frequency,

$$\omega_{ce} = \frac{eB}{mc} \text{ , and } \omega_{UH} = \sqrt{\omega_{pe}^2 + \omega_{ce}^2} .$$

Eq. (1) gives the well-known dispersion relation for the extraordinary wave. For laser pellet applications, $\omega_{ce} << \omega_0$, and the cut-off density n_{cut} (the density at which propagation cuts off for light waves incident from low density) is determined by $\omega_0^2 = \omega_{pe}^2 + \omega_{pe}\,\omega_{ce}$. Since $\omega_{ce} << \omega_0$, this cut-off density is only slightly less than the critical density n_{cr} (defined by $\omega_0 = \omega_{pe}$). For example, for $\omega_{ce}/\omega_0 = .04$, $n_{cut} = .96\, n_{cr}$.

As is apparent from Eq. (2), the extraordinary wave is partly longitudinal. This electrostatic field is simply the plasma response to the oscillation of electrons in the $\underline{v}_{os} \times \underline{B}_0$ force. Note that this field becomes infinite when $\varepsilon_2 = 0$, since the plasma response is then resonant. The resonance occurs at $n_R = n_{cr}$ $[1 - (\omega_{ce}/\omega_0)^2]$, which is essentially the critical density for $\omega_{ce} << \omega_0$. Physically, the light is reflected at the cut-off density ($n_{cut} < n_R$), but its electric field tunnels into the higher density region, where upper hybrid waves are resonantly driven. Of course, collisions, thermal corrections or non-linear effects keep the resonantly-driven field finite. For light intensities commonly used, E_z is limited by strong wave-breaking as will be shown in the simulations.

The principal features of this absorption mechanism can be obtained rather simply. Since $E_z \equiv E_d/\varepsilon_2$, the behavior of the electrostatic fields is determined by the value of the effective driver field E_d at the resonance point. To determine this driver field we need to estimate E_y at the resonance point. Assuming a locally linear density profile,[8] we first estimate E_y at the cut-off density by analogy to the well-known Airy function solution for the $B_o = 0$ case and then multiply by the exponential decay of the field to the resonance point. The result is

$$E_d \approx 1.3(k_o L)^{1/6} E_L \frac{\omega_{ce}}{\omega_o} e^{-\frac{\pi}{2} k_o L \left(\frac{\omega_{ce}}{\omega_o}\right)^{3/2}} , \qquad (5)$$

where L is the density scale length and k_o and E_L are the wave number and electric field of the light in vacuum. Although an improved value of E_d can be obtained by a detailed solution of Eq. (1) (as is done in the simulations), this simple estimate will suffice to illustrate some of the scalings which is our principal goal in this section.

Several results are now readily obtained. First, the maximum plasma wave amplitude as determined by wave breaking is

$$E_d \approx E_d' / \left(\sqrt{\frac{X_d}{L}} + \frac{\sqrt{[illegible]}\,\lambda_{De}}{L} \right) , \qquad (6)$$

where $X_d = \frac{eE_d}{m\omega_o^2}$ and λ_{De} is the electron Debye length. The second term in the denominator approximates a thermal correction to the cold plasma prediction. In addition, the absorption efficiency f is obtained by invoking energy balance

$$f \frac{cE_L^2}{8\pi} = \int dz \; \frac{\nu E_L^2(z)}{8\pi} ,$$

where ν is the magnitude of the plasma wave damping (either linear or nonlinear). As long as $\nu \ll \omega_o$, the integral is independent of the detailed value of ν (the height of the resonance is $\alpha\ 1/\nu$, and the width of the resonant region is $\alpha\nu$). Hence, we obtain

$$f \approx 5(k_o L)^{[illegible]/3} \left(\frac{\omega_{ce}}{\omega_o}\right)^{[illegible]} e^{-[illegible](k_o L)\left(\frac{\omega_{ce}}{\omega_o}\right)^{3/2}} . \qquad (7)$$

Defining $\beta \equiv (k_0L)^{1/3}\left(\frac{\omega_{ce}}{\omega_0}\right)^{1/2}$, we have $f \propto \beta^4 e^{-\pi\beta^3}$, and so the estimated absorption peaks at $\simeq$ 40% for $\beta \approx .8$. This behavior is easy to understand physically. As $\beta \to 0$ (for example, for $B_0 = 0$), the coupling goes to zero. For large β, the resonance point becomes inaccessible. For laser pellet applications, we will see that β can be $O(1)$ based on recent measurements of the magnitude of the self-generated magnetic fields.

It should be noted that the basic mechanism is linear, although the size of the self-generated magnetic field will depend on both the intensity and the uniformity of the irradiation. We also note that this mode conversion is operative whenever $\underline{E}_L \times \underline{B}_0 \neq 0$. In the toroidal fields due to $\nabla n \times \nabla T$ sources, the coupling then occurs at preferred locations in the focal spot. However, we emphasize that there are a number of other sources of magnetic fields which may change their spatial structure.

III. COMPUTER SIMULATIONS OF THE MODE CONVERSION

To test this coupling, we have carried out simulations using an electromagnetic, relativistic particle code.[14] In choosing the parameters of a representative simulation, we are principally motivated by the recent NRL work[1,2]; in particular, we choose, B_0 = 4 MG, $I = 10^{16}$ W/cm^2 (Nd light), and a rather short density gradient length ($L/\lambda_0 = 1.5$). Such a short gradient is also consistent with some recent measurements of the density scale lengths in laser-produced plasmas.[15] For simplicity we use a fixed, neutralizing ion background, since the basic mechanism is independent of ion motion. In the code, the light is normally incident on an inhomogeneous plasma slab. To model the dc magnetic fields shown by the fluid calculations, we simply impose a constant magnetic field orthogonal both to the density gradient and to the electric field vector of the incident light.

The strong plasma wave generation near the critical density is clearly shown in Fig. 1, which is an electron phase space plot from the simulation. The electrostatic field is clearly limited by wave breaking and reaches a peak value of $eE_p/m\omega_0 c \approx .15$. (The simple estimate in Eq. (6) predicts $eE_p/m\omega_0 c \approx .17$). The time-averaged laser light absorption measured in the simulation is $\approx$ 15%, also in reasonable agreement with the estimate given in Eq. (7) which is 16%. Although modest, this absorption does not require oblique incidence or p-polarization and hence will reduce the sensitivity of mode conversion to angle of incidence and polarization.

Finally, we have carried out a number of simulations varying both the density gradient and the size of the magnetic field.

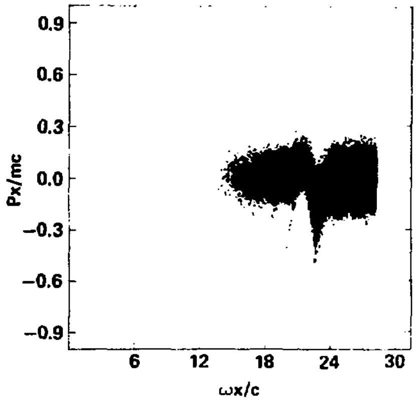

Fig. 1: A plot of electron phase space (p_x vs x) from the simulation at $\omega_c t$ = 125.2. The parameters are $eE_L/m\omega_0 c$ = .1, v_e/c = .1, $k_0 L$ = 10, ω_{ce}/ω_0 = .04 and fixed ions.

As shown in Fig. 2, the calculated electrostatic field is quite large and scales in reasonable agreement with the theoretical estimates. Such close agreement is probably fortuitous, since our theoretical estimates are rather crude. The absorptions measured in these short-time simulations also scale in reasonable agreement with the theoretical estimate. For example, when β = .6 we find an absorption of $\simeq$ 30% (the estimated value is $\approx$ 35%). We emphasize that both the actual scale lengths and the values of B_0 in experiments are not well-known and depend on such features as energy transport inhibition and the radial intensity profile of the light beam. The principal point is that for parameters characteristic of those recently measured, the self-generated magnetic field can introduce an interesting amount of absorption.

To further emphasize this point, let us compare the mode conversion introduced by a magnetic field with that introduced by oblique incidence. Comparing our results in Section II with similar estimates for the case of no magnetic field (but obliquely

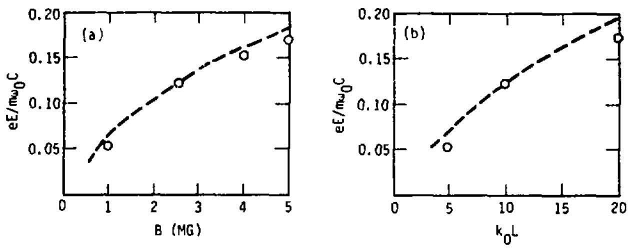

Fig. 2: The peak electrostatic field from the simulations as a function of a) the magnitude of the magnetic field ($k_0L=10$) and b) the density gradient scale length (B=2.5MG). The dashed line is our theoretical estimate. The parameters of the simulations are $eE_L/m\omega_0 c=.1$, $v_e/c=.1$ (v_e is the electron thermal velocity), and fixed ions.

incident p-polarized light), we readily see that the presence of the magnetic field corresponds to an angle of incidence of $\theta \simeq \sin^{-1} (\omega_{ce}/\omega_0)^{1/2}$. For example, for $\omega_{ce}/\omega_0 = .04$, $\theta \simeq 11°$. This is approximately the mean angle of incidence (averaged over energy) for light focused by an f/2 lens onto a planar target. Hence mode conversion due to a self-generated field can dominate that due to oblique incidence when large f number lenses are used (or when clam shells are used to focus light nearly normally onto spherical targets).

IV. SECOND HARMONIC GENERATION

Since the mode conversion gives rise to large electrostatic fields near the critical density, we can expect a sizeable level of second harmonic emission to occur. This emission can be simply computed by iterating the wave equation to obtain

$$\left(\frac{d^2}{dz^2} + \frac{4\omega_o^2}{c^2}\right) E_y^{(2)} = \frac{-4\omega_o^2}{c^2} \frac{4\pi}{2i\omega_o} J_y^{(2)}$$

where the superscripts refer to the component at frequency $2\omega_o$.

$$J_y^{(2)} = - n_o e v_y^{(2)} - n^{(1)} e v_y^{(1)} \quad ,$$

where n_o is the background density, $n^{(1)}$ the density fluctuation, and $v_y^{(1)}$ is the oscillation velocity of electrons in the transverse field. Using our crude estimate (Equation 5) for the effective driver, noting that $J_y^{(2)}$ is very peaked near the critical density, and taking the magnetic field as small, we obtain

$$\frac{E_y^{(2)}}{E_L} \sim 2.7 \left(\frac{eE_L}{m\omega_o c}\right) \left(k_o L\right)^{2/3} \beta^2 e^{-\pi\beta^3}$$

Here $E_y^{(2)}$ (E_L) is the amplitude of the backreflected second harmonic light (the incident laser light) in vacuum.

This simple estimate is compared with 1½ dimensional simulation results in Fig. 3. The dependence on both magnetic field

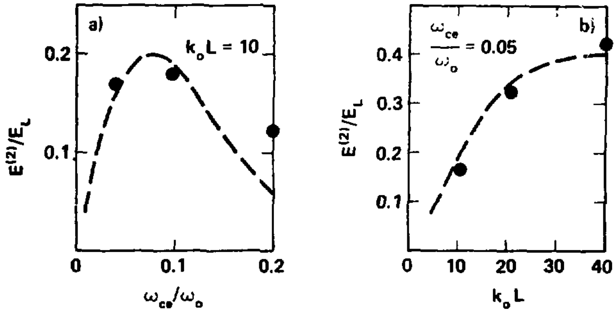

Fig. 3: The second harmonic field as a function of a) the magnetic field and b) the density scale length. The dashed line is a theoretical estimate. For these results a 1.5 dimensional code was used, $v_{os}/c=.1$, and $v_e/c = .09$.

and density scale length is in reasonable agreement. Note that the second harmonic emission can be quite large when the local scale length is long. However, with scale lengths more characteristic of steepened profiles, the energy in the second harmonic is of order 1% of the incident light energy. We note that a similar strong dependence of the magnitude of the second harmonic emission on local scale length has also been found[16] for the emission which accompanies resonance absorption of obliquely incident light. Hence the magnitude of the second harmonic emission provides an indirect indication of the local scale length near the critical density.

The reduction of the $2\omega_o$ emission by profile steepening suggests a simple explanation for some recent measurements at Limeil.[17] At low intensities the second harmonic emission was observed to increase in magnitude as the square of the incident light intensity. However, at a critical intensity of $\sim 5 \times 10^{13}$ W/cm^2 (Nd laser light), the dependence of this emission on intensity abruptly changed. Simple estimates show that this is just the intensity for which significant nonlinear profile steepening near the critical density is expected to onset and reduce the emission.

Finally the simulations also show that frequency structure in the second harmonic light may provide a diagnostic for the presence of large self-generated magnetic fields. As shown in Fig. 4, we observe a satellite line shifted down in frequency from $2\omega_o$ by an amount which is $\sim \omega_{ce}$. When the size of the magnetic field was doubled, the frequency shift became twice as large, confirming its dependence on B_o. Such frequency structure may arise, for example, from the coupling together of different Bernstein modes. An analytic theory of the structure should take into account finite larmor radius effects.

A magnetic field-induced line structure in the $2\omega_o$ light may indeed have been observed in the Limeil experiments.[17] A satellite line was observed shifted in frequency from the main line at $2\omega_o$ by an amount which was too large to be accounted for by an ion acoustic wave. If attributed to a magnetic field, the magnitude of the shift would correspond to a field of $\sim$ .5MG, which is a plausible value at the light intensity used in these experiments.

It is worth noting that self-generated magnetic fields can also account for a frequency splitting of the $3/2\ \omega_o$ light, which has been observed.[17,18] In simulations of stimulated scattering in underdense plasma with $n \lesssim .25\ n_{cr}$, we found that the incident light decayed into scattered light waves plus several different Bernstein modes. The result was a spectrum of electrostatic waves near $\omega_o/2$ but differing in frequency by an amount proportional to

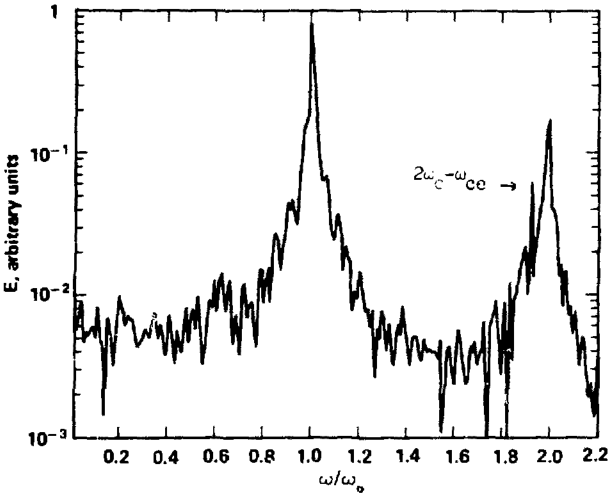

Fig. 4: The fourier-analyzed electric field of the incident and reflected light from a simulation using a 1½-D code. The parameters are v_{os}/c = .1, v_e/c=.09, ω_{ce}/ω_o =.1, and $k_o L$ = [illegible].

ω_{ce}. These electrostatic waves in turn can scatter the incident light to give a split line near $3/2\ \omega_o$.

V. SUMMARY

In conclusion, our calculations show that self-generated magnetic fields can play a significant role in laser plasma interactions. These fields introduce resonance absorption of even normally incident light and so can strongly reduce the dependence of linear mode conversion on angle of incidence and polarization. In addition, these magnetic fields provide an additional mechanism for second harmonic generation. Several features of this harmonic emission may provide indirect information about both the local density gradients and the size of the magnetic fields. More detailed calculations await a better understanding of the size and structure of the self-generated fields.

REFERENCES

1. B. H. Ripin et al., Phys. Rev. Letters [illegible], [illegible] (1975).

2. J. A. Stamper and B. H. Ripin, Phys. Rev. Letters 34, 138 ([illegible]); J. A. Stamper, K. Papadopoulos, R. N. Sudan, S. O. Dean, E. A. McLean, and J. M. Dawson, ibid 26, 1012 (1971).

3. J. B. Chase, J. M. LeBlanc, and J. R. Wilson, Phys. Fluids 16, [illegible] (1973).

4. R. [illegible], W. Mead, W. Kruer, L. Phillion, H. Kornblum, J. Lindl, [illegible], V. Rupert, and K. Tirsell, Phys. Fluids (in press).

5. [illegible] and [illegible], Phys. Rev. Letters [illegible], [illegible] ([illegible]); [illegible] A. [illegible] and [illegible] A. [illegible], Phys. Fluids 17, [illegible] ([illegible]).

6. J. J. Thomson, C. E. Max, and K. G. Estabrook, Phys. Rev. Letters [illegible], [illegible] ([illegible]).

7. E. Lindman, D. Forslund, J. Kindel, K. Lee, and W. Shanahan, Bull. Am. Phys. Soc. [illegible], [illegible] (1975).

8. G. H. Dahlbacka, W. C. Mead, C. E. Max, and J. J. Thomson, Lawrence Livermore Laboratory Report UCRL-77150 (1975).

9. V. L. Ginzburg, The Propagation of Electromagnetic Waves in Plasmas (Pergamon Press, London, 1965), Chs. 4 and 5.

10. J. P. Freidberg, R. W. Mitchell, R. L. Morse, and L. I. Rudinski, Phys. Rev. Letters 28, 795 ([illegible]); D. Forslund, J. M. Kindel, and E. L. Lindman, Phys. Rev. A 11, 679 (1975); K. G. Estabrook, E. J. Valeo, and W. L. Kruer, Phys. Fluids 18, 1151 (1975).

11. J. S. DeGroot and J. Tull, Phys. Fluids 18, 672 (1975); P. Koch and J. Albritton, Phys. Rev. Letters 32, 1420 (1975).

12. T. Stix, Phys. Rev. Letters 6, 878 (1965).

13. J. J. Schuss and J. C. Hosea, Phys. Fluids 18, 727 (1945).

14. A. B. Langdon and B. F. Lasinski, in Methods in Computational Physics, edited by J. Killeen, B. Alder, S. Fernbach, and M. Rotenberg (Academic, New York), Vol. 16, 327-365 (1976).

15. T. P. Donaldson and I. J. Spalding, Phys. Rev. Letters 36, 467 (1976).

16. N. S. Erokhin, S. S. Moiseev, V. V. Mukhin, Nuclear Fusion 14, 333 (1974); K. Eidmann and R. Sigel, Physical Review Letters 34, 799 (1975).

17. J. L. Bobin, in Proceedings of the Nobel Symposium, edited by H. Wilhelmsson (Plenum Press, London) in press.

18. H. C. Pant, K. Eidmann, P. Sachsenmaier, and R. Sigel, Optics Comm. 16, 396 (1976).